

# 192892: mafic granulite, Lucy Hill

(*Youanmi Terrane, Yilgarn Craton*)

Blereau, ER, Korhonen, FJ and Kelsey, DE

## Location and sampling

HYDEN (SI 50-4), HURLSTONE (2732)

MGA Zone 50, 723495E 6384109N

Warox Site FJKBGD192892

Sampled on 18 May 2009

This sample was collected from an outcrop on the south side of Lucy Hill, along the north side of the Hyden – Lake King Road, about 3.5 km northwest of Holt Rock and 2.7 km southeast from the junction with Di Russo Road. The sample was collected as part of the Yilgarn Craton Metamorphic Project (2003–14) undertaken by Ben Goscombe for the Geological Survey of Western Australia (GSA), and referred to in that study as sample BG09-145a. The results from this project have not been released by GSA, although select data have been published in Goscombe et al. (2019). This sample is not available in the GSA collections; all observations are based on descriptions presented in Goscombe et al. (2019) and have not been directly verified.

## Geological context

The unit sampled is a mafic granulite of the western Youanmi Terrane (Quentin de Gromard et al., 2021). This unit is part of a belt of Archean metasedimentary and gneissic rocks previously assigned to the South West Terrane and referred to informally by Wilde and Pidgeon (1987) as the ‘Wheat Belt’ region (cf. Wilde, 2001). However, a recent reinterpretation places the boundary between the South West and the Youanmi Terranes farther to the southwest than shown on older maps (Quentin de Gromard et al., 2021). The Youanmi Terrane contains both granite–greenstone and high-grade gneiss components with emplacement ages from 3010 to 2600 Ma (GSA, 2020; Cassidy et al., 2006). Existing geochronological data from this part of the Youanmi Terrane is sparse. A biotite metagranodiorite, collected about 109 km to the south-southeast of this locality, yielded an igneous crystallization age of  $2978 \pm 5$  Ma (GSA 224357, Lu et al., 2018). Two samples of garnet-bearing alkali feldspar granite from Griffins Find about 109 km to the west-southwest yielded crystallization ages of c. 2636 Ma (Qiu and McNaughton, 1999). A quartzite also collected from Griffins Find yielded detrital zircon dates between c. 3812 and 2643 Ma, and a conservative maximum age of deposition of  $2655 \pm 11$  Ma (GSA 198580, Lu et al., 2015b). A pelitic gneiss from Griffins Find yielded detrital zircon dates between c. 2838 and 2629 Ma, and a conservative maximum depositional age of  $2638 \pm 2$  Ma (GSA 198578; Lu et al., 2015a), and another pelitic gneiss sample yielded a monazite age for high-grade metamorphism of  $2641 \pm 6$  Ma (GSA 198585, Fielding et al., 2021).

## Petrographic description

The sample is a massive medium- to coarse-grained mafic granulite containing green–brown hornblende, clinopyroxene, plagioclase and ilmenite (Fig. 1). Titanite and quartz may be present but have not been verified. The sample has a weak grain-shape fabric and a polygonal granoblastic matrix. It is unknown whether the sample has undergone partial melting. Mineral compositions are provided in Table 1.

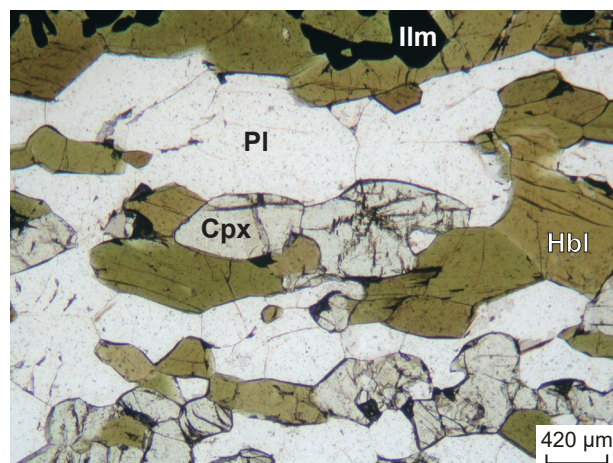


Figure 1. Photomicrograph of sample 192892: mafic granulite, Lucy Hill in plane-polarized light. Mineral abbreviations are explained in the caption to Figure 2

Table 1. Mineral compositions for sample 192892: mafic granulite, Lucy Hill

Mineral <sup>(a)</sup>	Hbl	Hbl	Cpx	Cpx	Pl	Pl	Ilm
Setting	Core	Rim	Core	Rim	Core	Rim	Matrix
<i>wt%</i>							
SiO <sub>2</sub>	44.23	44.28	51.35	51.18	56.15	55.37	0.05
TiO <sub>2</sub>	1.88	1.71	0.15	0.19	0.02	0.00	49.59
Al <sub>2</sub> O <sub>3</sub>	9.06	9.01	1.38	1.32	26.02	26.01	0.00
Cr <sub>2</sub> O <sub>3</sub>	0.00	0.00	0.00	0.00	0.00	0.00	0.00
FeO	14.30	14.52	9.95	10.11	0.13	0.18	47.90
MnO	0.15	0.23	0.37	0.36	0.00	0.00	0.74
MgO	12.78	12.86	13.41	13.38	0.00	0.00	1.01
ZnO	0.00	0.02	0.05	0.00	0.04	0.00	0.08
CaO	11.10	11.36	21.76	21.90	8.68	9.01	0.00
Na <sub>2</sub> O	1.76	1.61	0.34	0.36	6.44	6.29	0.02
K <sub>2</sub> O	0.72	0.81	0.02	0.01	0.32	0.32	0.03
Total <sup>(b)</sup>	95.99	96.38	98.73	98.81	97.77	97.17	99.35
Oxygen	23	23	6	6	8	8	3
Si	6.56	6.55	1.94	1.94	2.57	2.55	0.00
Ti	0.21	0.19	0.00	0.01	0.00	0.00	0.94
Al	1.58	1.57	0.06	0.06	1.40	1.41	0.00
Cr	0.00	0.00	0.00	0.00	0.00	0.00	0.00
Fe <sup>3+(c)</sup>	0.74	0.78	0.07	0.09	0.00	0.00	0.13
Fe <sup>2+</sup>	1.04	1.02	0.24	0.23	0.01	0.01	0.88
Mn <sup>2+</sup>	0.02	0.03	0.01	0.01	0.00	0.00	0.02
Mg	2.83	2.84	0.76	0.75	0.00	0.00	0.04
Zn	0.00	0.00	0.00	0.00	0.00	0.00	0.00
Ca	1.76	1.80	0.88	0.89	0.43	0.45	0.00
Na	0.51	0.46	0.03	0.03	0.57	0.56	0.00
K	0.14	0.15	0.00	0.00	0.02	0.02	0.00
Total	15.39	15.39	4.00	4.00	5.00	5.00	2.00
<i>Compositional variables</i>							
XFe <sup>(d)</sup>	0.27	0.26	0.24	0.24	–	–	0.96

NOTES: – not applicable  
 (a) Mineral abbreviations explained in the caption to Figure 2  
 (b) Totals on anhydrous basis  
 (c) Hornblende cations calculated following Holland and Blundy (1994); Fe<sup>3+</sup> contents for other minerals based on Droop (1987)  
 (d) XFe = Fe<sup>2+</sup>/(Fe<sup>2+</sup> + Mg)

## Analytical details

Preliminary  $P$ – $T$  estimates were obtained using multiple-reaction thermobarometry calculated from the mineral compositions (Table 1; Goscombe et al., 2019). These estimates were derived from the ‘averagePT’ module (avPT) in the program THERMOCALC version tc325 (Powell and Holland, 1988), using the internally consistent Holland and Powell (1998) dataset.

The metamorphic evolution of this sample has been subsequently re-evaluated using phase equilibria modelling, based on the bulk-rock composition (Table 2). The bulk-rock composition was determined by X-ray fluorescence spectroscopy, together with loss on ignition (LOI). The modelled O content (for  $\text{Fe}^{3+}$ ) was set to be 20% of the measured total Fe; the modelled  $\text{H}_2\text{O}$  content was the measured LOI. The bulk composition was adjusted for the presence of apatite by applying a correction to CaO (Table 1). Thermodynamic calculations were performed in the NCKFMASHTO ( $\text{Na}_2\text{O}$ – $\text{CaO}$ – $\text{K}_2\text{O}$ – $\text{FeO}$ – $\text{MgO}$ – $\text{Al}_2\text{O}_3$ – $\text{SiO}_2$ – $\text{H}_2\text{O}$ – $\text{TiO}_2$ – $\text{O}$ ) system using THERMOCALC version tc340 (Powell and Holland, 1988; updated October 2013) and the internally consistent thermodynamic dataset of Green et al. (2016; version dataset tc-ds63, created January 2015). The activity–composition relations used in the modelling are detailed in Green et al. (2016), with the augite model used for clinopyroxene. Additional information on the workflow with relevant background and methodology are provided in Korhonen et al. (2020).

**Table 2. Measured whole-rock and modelled compositions for sample 192892: mafic granulite, Lucy Hill**

<i>XRF whole-rock composition (wt%)<sup>(a)</sup></i>												
<b>SiO<sub>2</sub></b>	<b>TiO<sub>2</sub></b>	<b>Al<sub>2</sub>O<sub>3</sub></b>	<b>Fe<sub>2</sub>O<sub>3</sub><sup>(b)</sup></b>	<b>FeO<sup>(b)</sup></b>	<b>MnO</b>	<b>MgO</b>	<b>CaO</b>	<b>Na<sub>2</sub>O</b>	<b>K<sub>2</sub>O</b>	<b>P<sub>2</sub>O<sub>5</sub></b>	<b>LOI</b>	<b>Total</b>
54.08	0.44	13.22	–	7.32	0.14	7.33	11.63	3.05	0.42	0.03	0.54	98.20
<i>Normalized composition used for phase equilibria modelling (mol%)</i>												
<b>SiO<sub>2</sub></b>	<b>TiO<sub>2</sub></b>	<b>Al<sub>2</sub>O<sub>3</sub></b>	<b>O<sup>(c)</sup></b>	<b>FeO<sup>T(d)</sup></b>	<b>MnO</b>	<b>MgO</b>	<b>CaO<sup>(e)</sup></b>	<b>Na<sub>2</sub>O</b>	<b>K<sub>2</sub>O</b>	<b>–</b>	<b>H<sub>2</sub>O<sup>(f)</sup></b>	<b>Total</b>
55.98	0.34	8.06	0.57	5.70	–	11.31	12.85	3.06	0.27	–	1.86	100

**NOTES:** (a) Data and analytical details are available from the WACHEM database <<http://geochem.dmp.wa.gov.au/geochem/>>  
 (b) FeO content is total Fe  
 (c) O content (for  $\text{Fe}_2\text{O}_3$ ) set to be 20% of measured  $\text{FeO}^{(b)}$   
 (d)  $\text{FeO}^T$  = moles  $\text{FeO} + 2 * \text{moles O}$   
 (e) CaO modified to remove apatite:  $\text{CaO}(\text{Mod}) = \text{CaO}(\text{Total}) - (\text{moles CaO}(\text{in Ap}) = 3.33 * \text{moles P}_2\text{O}_5)$   
 (f)  $\text{H}_2\text{O}$  content is the measured LOI  
 – not applicable

## Results

The  $P$ – $T$  pseudosection for sample 192892 was calculated over a  $P$ – $T$  range of 2–8 kbar and 650–900 °C (Fig. 2). The solidus is located between 745 and 810 °C across the range of modelled pressures. Garnet is stable above 7.4 kbar at 650 °C and rutile is stable above 7 kbar at 800 °C. Orthopyroxene-absent assemblages are predicted between 720 and 860 °C across the range of modelled pressures. At temperatures above the solidus, orthopyroxene is restabilized, followed by the loss of quartz and hornblende as temperature increases.

Metamorphic  $P$ – $T$  estimates ( $\pm 2\sigma$  uncertainty) calculated using multiple-reaction thermobarometry are  $4.2 \pm 0.5$  kbar and  $712 \pm 25$  °C (Goscombe et al., 2019). These calculations used the core compositions (Table 1) to estimate peak conditions.

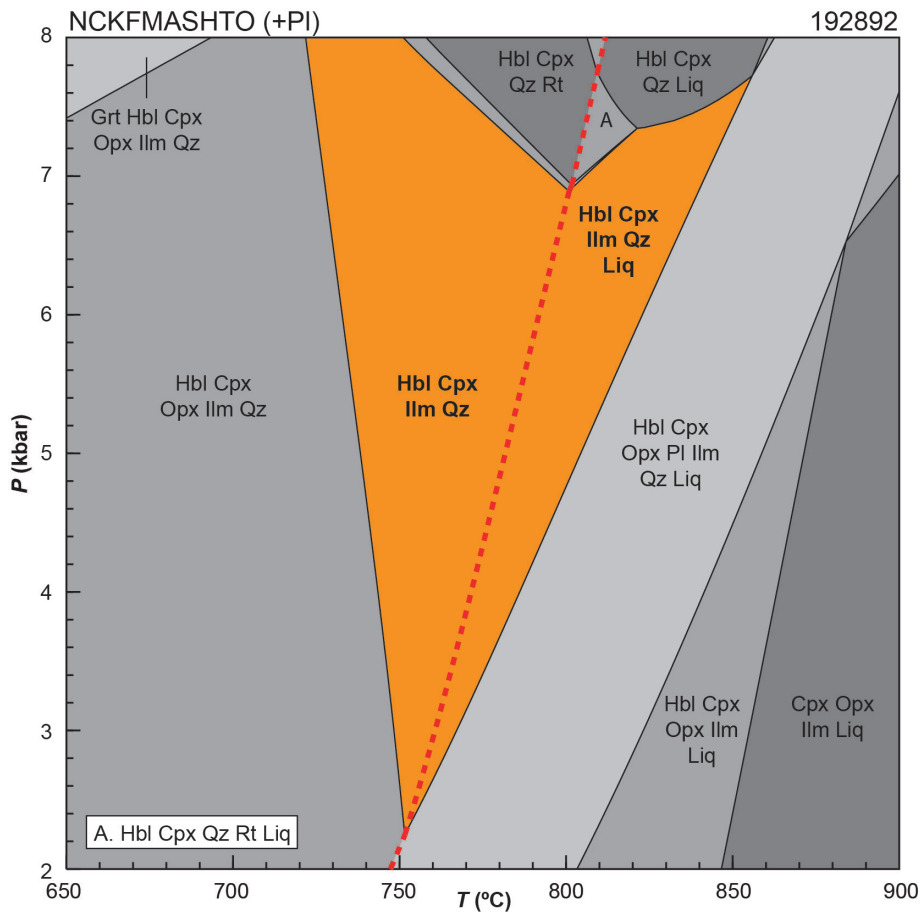


**Figure 2.** *P*–*T* pseudosection calculated for sample 192892: mafic granulite, Lucy Hill. Assemblage fields corresponding to peak metamorphic conditions are delimited by bold text and orange shading. Red dashed line represents the solidus. Abbreviations: Cpx, clinopyroxene; Grt, garnet; Hbl, hornblende; Ilm, ilmenite; Liq, silicate melt; Opx, orthopyroxene; Pl, plagioclase; Qz, quartz; Rt, rutile

## Interpretation

The peak metamorphic assemblage is interpreted to be hornblende–clinopyroxene–plagioclase–ilmenite–quartz(–melt). There is uncertainty whether the sample has undergone partial melting. The subsolidus hornblende–clinopyroxene–plagioclase–ilmenite–quartz field is stable between 720 and 800 °C from 2.2 to pressures above 8 kbar, and the melt-bearing field is stable between 750 and 855 °C at 2.2 – 7.7 kbar (Fig. 2). Both fields are delimited by the stability of orthopyroxene at lower pressure and lower and higher temperatures, and the stability of rutile and absence of ilmenite at higher pressure.

The results determined from multiple-reaction thermobarometry are at lower *P*–*T* conditions than the calculated stability of the peak hornblende–clinopyroxene–plagioclase–ilmenite–quartz(–melt) fields. There is no information on the prograde and retrograde segments of the *P*–*T* path, and therefore the overall shape of the *P*–*T* path is not defined.

Based on the results of phase equilibria modelling, peak metamorphic conditions are poorly constrained, with estimates between 720–855 °C and 2.2 – 8 kbar. Mineral compositions are consistent with equilibration at  $712 \pm 25$  °C,  $4.2 \pm 0.5$  kbar, defining an apparent thermal between 150 and 190 °C/kbar.

## References

- Cassidy, KF, Champion, DC, Krapež, B, Barley, ME, Brown, SJA, Blewett, RS, Groenewald, PB and Tyler, IM 2006, A revised geological framework for the Yilgarn Craton, Western Australia: Geological Survey of Western Australia, Record 2006/8, 8p.
- Droop, GTR 1987, A general equation for estimating Fe<sup>3+</sup> concentrations in ferromagnesian silicates and oxides from microprobe analyses, using stoichiometric criteria: *Mineralogical Magazine*, v. 51, no. 361, p. 431–435.
- Fielding, IOH, Wingate, MTD, Korhonen, FJ and Rankenburg, K 2021, 198585: pelitic gneiss, Griffins Find; *Geochronology Record 1767*: Geological Survey of Western Australia, 5p.
- Geological Survey of Western Australia 2020, Youanmi, 2020: Geological Survey of Western Australia, Geological Information Series, digital data package.
- Goscombe, B, Foster, DA, Blewett, R, Czarnota, K, Wade, B, Groenewald, B and Gray, D 2019, Neoproterozoic metamorphic evolution of the Yilgarn Craton: a record of subduction, accretion, extension and lithospheric delamination: *Precambrian Research*, article no. 105441, doi:10.1016/j.precamres.2019.105441.
- Green, ECR, White, RW, Diener, JFA, Powell, R, Holland, TJB and Palin, RM 2016, Activity-composition relations for the calculation of partial melting equilibria in metabasic rocks: *Journal of Metamorphic Geology*, v. 34, no. 9, p. 845–869.
- Holland, T and Blundy, J 1994, Non-ideal interactions in calcic amphiboles and their bearing on amphibole-plagioclase thermometry: *Contributions to Mineralogy and Petrology*, v. 116, no. 4, p. 433–447.
- Holland, TJB and Powell, R 1998, An internally consistent thermodynamic data set for phases of petrological interest: *Journal of Metamorphic Geology*, v. 16, no. 3, p. 309–343.
- Korhonen, FJ, Kelsey, DE, Fielding, IOH and Romano, SS 2020, The utility of the metamorphic rock record: constraining the pressure–temperature–time conditions of metamorphism: *Geological Survey of Western Australia, Record 2020/14*, 24p.
- Lu, Y, Wingate, MTD, Kirkland, CL, Goscombe, B and Wyche, S 2015a, 198578: pelitic gneiss, Griffins Find; *Geochronology Record 1284*: Geological Survey of Western Australia, 4p.
- Lu, Y, Wingate, MTD, Kirkland, CL, Goscombe, B and Wyche, S 2015b, 198580: quartzite, Griffins Find; *Geochronology Record 1285*: Geological Survey of Western Australia, 5p.
- Lu, Y, Wingate, MTD and Smithies, RH 2018, 224357: biotite metagranodiorite, Phillips River; *Geochronology Record 1550*: Geological Survey of Western Australia, 4p.
- Powell, R and Holland, TJB 1988, An internally consistent dataset with uncertainties and correlations: 3. Applications to geobarometry, worked examples and a computer program: *Journal of Metamorphic Geology*, v. 6, no. 2, p. 173–204.
- Qiu, Y and McNaughton, NJ 1999, Source of Pb in orogenic lode-gold mineralisation: Pb isotope constraints from deep crustal rocks from the southwestern Archaean Yilgarn Craton, Australia: *Mineralium Deposita*, v. 34, p. 366–381.
- Quentin de Gromard, R, Ivanic, TJ and Zibra, I 2021, Interpreted bedrock geology of the southwest Yilgarn Craton: Geological Survey of Western Australia, in press.
- Wilde, SA 2001, *Jimperding and Chittering metamorphic belts, Western Australia - a field guide*: Geological Survey of Western Australia, Record 2001/12, 24p.
- Wilde, SA and Pidgeon, RT 1987, U–Pb geochronology, geothermometry and petrology of the main areas of gold mineralization in the ‘Wheat Belt’ region of Western Australia: *Western Australian Minerals and Petroleum Research Institute; Project 30, Final Report*, 171p.

## Links

Metamorphic history introduction document: [Intro\\_2020.pdf](#)

## Recommended reference for this publication

Blereau, ER, Korhonen, FJ and Kelsey DE 2021, 192892.1: mafic granulite, Lucy Hill; *Metamorphic History Record 6*: Geological Survey of Western Australia, 6p.

Data obtained: 19 May 2020

Date released: 25 June 2021

**This Metamorphic History Record was last modified on 9 June 2021.**

---

Grid references in this publication refer to the Geocentric Datum of Australia 1994 (GDA94). All locations are quoted to at least the nearest 100 m.

WAROX is GSWA's field observation and sample database. WAROX site IDs have the format 'ABCXXXnnnnnnSS', where ABC = geologist username, XXX = project or map code, nnnnnn = 6 digit site number, and SS = optional alphabetic suffix (maximum 2 characters).

Isotope and element analyses are routinely conducted using the GeoHistory laser ablation ICP-MS and Sensitive High-Resolution Ion Microprobe (SHRIMP) ion microprobe facilities at the John de Laeter Centre (JdLC), Curtin University, with the financial support of the Australian Research Council and AuScope National Collaborative Research Infrastructure Strategy (NCRIS). The TESCAN Integrated Mineral Analyser (TIMA) instrument was funded by a grant from the Australian Research Council (LE140100150) and is operated by the JdLC with the support of the Geological Survey of Western Australia, The University of Western Australia (UWA) and Murdoch University. Mineral analyses are routinely obtained using the electron probe microanalyser (EPMA) facilities at the Centre for Microscopy, Characterisation and Analysis at UWA, and at Adelaide Microscopy, University of Adelaide.

Digital data related to WA Geology Online, including geochronology and digital geology, are available online at the Department's [Data and Software Centre](#) and may be viewed in map context at [GeoVIEW.WA](#).

#### **Disclaimer**

This product uses information from various sources. The Department of Mines, Industry Regulation and Safety (DMIRS) and the State cannot guarantee the accuracy, currency or completeness of the information. Neither the department nor the State of Western Australia nor any employee or agent of the department shall be responsible or liable for any loss, damage or injury arising from the use of or reliance on any information, data or advice (including incomplete, out of date, incorrect, inaccurate or misleading information, data or advice) expressed or implied in, or coming from, this publication or incorporated into it by reference, by any person whatsoever.



© State of Western Australia (Department of Mines, Industry Regulation and Safety) 2021

With the exception of the Western Australian Coat of Arms and other logos, and where otherwise noted, these data are provided under a Creative Commons Attribution 4.0 International Licence. (<http://creativecommons.org/licenses/by/4.0/legalcode>)

#### **Further details of geoscience products are available from:**

Information Centre

Department of Mines, Industry Regulation and Safety

100 Plain Street

EAST PERTH WA 6004

Telephone: +61 8 9222 3459 | Email: [publications@dmirs.wa.gov.au](mailto:publications@dmirs.wa.gov.au)

[www.dmirs.wa.gov.au/GSWApublications](http://www.dmirs.wa.gov.au/GSWApublications)